CFD Study on Flow Distribution at the Core Inlet Region of SMART

Youngmin Bae[a,*], Hongyun So[a], Yu Mi Jeon[a], Yeong-Gil Kim[a], Young-In Kim[a], Cheon-Tae Park[a], Suhn Choi[a]
[a]*Korea Atomic Energy Research Institute, 1045 Daedeok Street, Yuseong-gu, Daejeon, 305-353, Korea*
[*]*Corresponding author: ybae@kaeri.re.kr*

1. Introduction

With recent advances in computing resources, computational fluid dynamics (CFD) approach has been widely used in many practical applications for nuclear power plants. For instance, CFD methodology has received great attention from the researcher to investigate thermal-hydraulic characteristics in fuel rod bundles [1,2] and to improve the design process for reactor internals [3,4]. In this paper, we numerically investigate the flow distribution at the core inlet region, which is expected to play an important role in core heat removal. The influences of computational mesh and turbulence model are also evaluated for a validation of CFD model.

2. Methods and Results

2.1 Description of CFD model

In the present study, a commercial CFD code, Fluent 12.0 was utilized for three-dimensional, incompressible, and turbulent flow analysis [5], which is governed by

$$\frac{\partial \langle u_i \rangle}{\partial x_i} = 0 \tag{1}$$

$$\rho \frac{\partial \langle u_i \rangle \langle u_j \rangle}{\partial x_j} = -\frac{\partial \langle p \rangle}{\partial x_i} + \frac{\partial}{\partial x_j}\left[\mu \left(\frac{\partial \langle u_i \rangle}{\partial x_j} + \frac{\partial \langle u_j \rangle}{\partial x_i} \right) - \rho \langle u_i' u_j' \rangle \right] \tag{2}$$

Figure 1 illustrates a typical computational domain used in the simulation and corresponding boundary conditions. The domain includes the fuel assemblies, flow skirt (FS) which has hundreds of small flow holes, lower core support plate (LCSP) having four flow holes at every fuel assembly. In all simulations, the fuel assemblies are simply modeled as a porous medium because the flow distribution in the core inlet region is of our interest. The steady-state simulations are carried out with segregated and double precision solver, SIMPLE algorithm for pressure-velocity coupling, second order upwind method for discretization, and standard wall function for near wall treatment (without low Reynolds correction for SST k-ω turbulence model), while water with constant density and viscosity was used as working fluid. Table 1 summarizes the computational setup for several test cases.

Table 1. Summary of simulation cases

Case	Mesh number	Turbulence model	Mass flow rate (m/m_{ref})	
			Inlet1	Inlet2
I	86.6 M	SST k-ω	1	-
II	43.8 M	SST k-ω	1	-
III	43.8 M	Realizable k-ε	1	-
IV	87.6 M	SST k-ω	1	1
V	87.6 M	SST k-ω	1.3	0.7
VI	87.6 M	Realizable k-ε	1.3	0.7

2.2 Grid sensitivity and influence of turbulence model

Two different mesh resolutions, i.e. 86.6 million cells for fine grid (Case I) and 43.8 million hexahedral cells for coarse grid (Case II and Case III), are attempted for grid dependency test. The computational grids are clustered at the walls and around the flow holes in the LCSP, at which the maximum y^+ values are set to 400 and 200 for coarse and fine grids, respectively. Also note that in grid dependency test, the CFD model contains only a 45° (or 1/8) segment of the geometry and the mass flow rate is uniform at the upstream.

Figure 2 compares the mass flow rates at the top of the LCSP. The difference of core mass flow rate between the two mesh densities is found to be less than 1%, and the test results are hardly changed by a further grid refinement. In addition, realizable k-ε and SST k-ω turbulence models give a very similar flow distribution with a maximum difference of 1.3% (not shown here). It is also seen in Fig. 2 that in both mesh densities, the deviation of mass flow rate between the

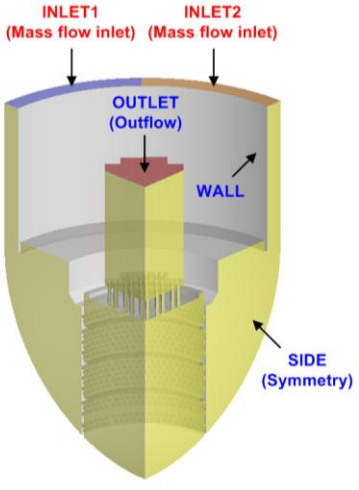

Fig. 1. Schematic of computational domain

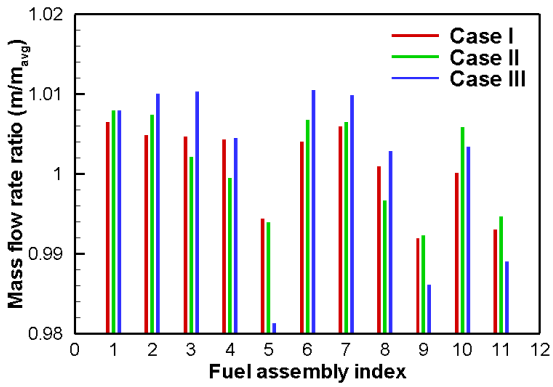

Fig. 2. Mass flow rate distribution at the top of LCSP

fuel assemblies does not exceed 2%. This is the case for different turbulence models, implying the present configuration of LCSP effectively distributes the flow at the core inlet region.

2.3 Flow distribution at non-uniform inflow condition

In order to investigate the flow distribution at the core inlet region further, we additionally consider the non-uniform upstream boundary condition which is very conservative in SMART. In these cases, the computational domain includes a quarter (or 90° segment) of the reactor geometry, and inlet plane is divided into two sub-parts on which either the same (Case IV) or different (Case V and Case VI) mass flow rates are given. The optimum mesh was chosen from the above grid dependency test, so it has 87.6 million volume cells. Two different turbulence models are also tested here, to evaluate any possible errors associated with turbulence models.

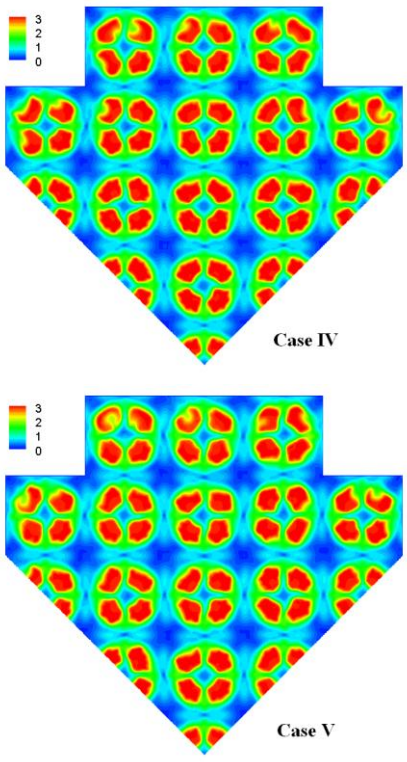

Fig. 3. Velocity magnitude contour at the core inlet

Figure 3 plots the velocity contours on the horizontal cross-section of the core inlet. It is shown that the almost identical flow distribution is revealed for Case IV and Case V. When non-uniform mass flow rate (±30% deviation) was imposed on the upstream, the maximum deviation of mass flow rate at the core inlet region is predicted to be slightly increased to 2.3%. The deviations associated with turbulence model remains less than 1% at the bottom of the core. These results consequently indicate that the uniform flow distribution at the core inlet region of SMART is successfully accomplished by the LCSP, even at the conservative upstream condition.

3. Conclusions

In this study, we investigated the flow distribution at the core inlet region of SMART. The three-dimensional incompressible turbulent flow was predicted by the commercial CFD code, Fluent 12.0 with different mesh resolutions, turbulence models and inflow conditions. In the test results, the maximum deviation of mass flow rate at core inlet region is predicted to be less than 2% and 2.3% at uniform and non-uniform upstream conditions, respectively. This indicates that the present LCSP effectively distributes the flow at the core inlet region of SMART, even in the case that the flow discharged from the upstream has certain degree of non-uniformity.

Acknowledgement

This study has been performed under a contract with the Korean Ministry of Educational Science and Technology.

REFERENCES

[1] S. Tóth, A. Aszódi, CFD Study on Coolant Mixing in VVER-440 Fuel Rod Bundles and Fuel Assembly Heads, Nuclear Engineering and Design, Vol. 240, pp. 2194-2205, 2010.
[2] C. C. Liu, Y. M. Ferng, Numerically Simulating the Thermal-Hydraulic Characteristics within the Fuel Rod Bundle using CFD Methodology, Nuclear Engineering and Design, Vol. 240, pp. 3078-3086, 2010.
[3] J. Yan, K. Yuan, E. Tatli, D. Huegel, Z. Karoutas, CFD Prediction of Pressure Drop for the Inlet Region of a PWR Fuel Assembly, CFD for Nuclear Reactor Safety Applications (CFD4NRS-3) Workshop, Sep. 14-16, 2010, Bethesda, MD.
[4] M. E. Conner, E. Baglietto, A. M. Elmahdi, CFD Methodology and Validation for Single-Phase Flow in PWR Fuel Assemblies, Nuclear Engineering and Design, Vol. 240, pp. 2088-2095, 2010.
[5] ANSYS Inc., Fluent 12.0 Manual, 2009.